JOURNAL OF MATERIALS SCIENCE 20 (1985) 845–853

Ferromagnetic resonance study of structural relaxation and crystallization of the Metglas 2826A amorphous alloy

R. S. DE BIASI, R. W. D. RODRIGUES
Centro de Pesquisa de Materiais, Instituto Militar de Engenharia, 22290 Rio de Janeiro, Brasil

The ferromagnetic resonance technique was used to study the ageing behaviour of the metallic glass $Fe_{32}Ni_{36}Cr_{14}P_{12}B_6$ (Metglas 2826A). The peak-to-peak linewidth was measured for several isothermal annealing times in the temperature range 350 to 375° C. After an initial decrease, attributed to structural relaxation, the linewidth increases linearly with the transformed fraction of the first crystallization phase. For $0.05 < f < 0.50$, the transformed fraction, f, as a function of time, t, satisfies the Avrami equation with the exponent n being between 1.58 and 1.71. The activation energy for the first crystallization phase is estimated from the times to reach 5 to 40% transformation to be 306 kJ mol^{-1}. The experimental results suggest that the second phase of crystallization begins when the transformed fraction of the first phase is of the order of 50%.

1. Introduction

The thermal stability of metallic glasses is a subject of practical interest, because temperature-induced structural changes may affect the performance of these engineering materials. Ferromagnetic resonance (FMR) spectroscopy seems to be a convenient method of observing these changes, because it is a fast, sensitive and non-destructive technique.

In the present work, the FMR technique was used to investigate the annealing behaviour of the commercial alloy Metglas 2826A ($Fe_{32}Ni_{36}Cr_{14}P_{12}B_6$), manufactured by Allied Chemical Corporation. The purpose of this study is two-fold: First, to assess the usefulness of the method, when applied to this particular system; second, to obtain new data about the relaxation and crystallization kinetics of the alloy.

2. Theory

The FMR parameters of a crystalline, ferromagnetic sample are related to the Landau–Lifshitz equation [1]

$$\frac{d\boldsymbol{M}}{dt} = -\gamma(\boldsymbol{M} \times \boldsymbol{H}) - \frac{\lambda}{M_s^2}[\boldsymbol{M} \times (\boldsymbol{M} \times \boldsymbol{H})], \quad (1)$$

where $\boldsymbol{M}$ is the magnetization vector, $\gamma = ge/2m$ the gyromagnetic ratio, λ the relaxation frequency and M_s the saturation magnetization. The peak-to-peak linewidth of the first-derivative FMR adsorption curve, calculated by solving Equation 1, is given by [2]

$$\Delta H_{LL} = \frac{4\pi}{\sqrt{3}} \frac{\lambda \nu}{\gamma^2 M_s}, \quad (2)$$

where ν is the microwave frequency.

In the case of amorphous alloys [3], a frequency-independent term, ΔH_I, due to the inhomogeneity of the internal magnetic field, must be included in Equation 2. In annealed metallic glasses, this term is related to two processes [4, 5]: (a) for small ageing times, the magnetic dipoles in the sample are reoriented, through a magnetostriction effect, towards a lower energy configuration which corresponds to a more homogeneous distribution of magnetic dipoles than in the virgin sample; as a consequence, ΔH_I decreases; (b) for longer ageing times, crystallization nuclei start to form and to grow; the internal field becomes less homogeneous and ΔH_I increases.

It has been observed experimentally [3] that the linewidths caused by relaxation broadening,

0022–2461/85 $03.00 + .12

ΔH_{LL}, and inhomogeneity broadening, ΔH_I, are additive. In other words, the measured linewidth may be expressed as

$$\Delta H_{pp} = \Delta H_{LL} + \Delta H_I. \quad (3)$$

From the preceding discussion it follows that the linewidth caused by inhomogeneity broadening, ΔH_I, should reflect any temperature-induced structural changes occurring in the sample. In this work, we used this fact to investigate the annealing behaviour of the Metglas 2826A alloy.

3. Experimental procedure

All the measurements reported in this study were obtained using samples cut from a ribbon (2 mm wide × 70 μm thick) of Metglas 2826A alloy with the composition $Fe_{32}Ni_{36}Cr_{14}P_{12}B_6$. Isothermal heat treatments were carried out by immersing small pieces of the ribbon (2 to 4 mm long) in a salt bath, with the temperature controlled to ± 0.5° C, followed by a water quench.

FMR measurements were performed at 77 K, because the alloy is paramagnetic at room temperature ($T_c = -19°$ C) [6]. The samples were mounted at the tip of a quartz tube, which was immersed in a liquid nitrogen bath. All measurements were taken with the static field parallel to the sample surface and along the long axis of the ribbon.

First-derivative FMR spectra were recorded at 9.5 GHz using an X-band Varian E-12 spectrometer. The magnetic field was calibrated with a proton resonance gaussmeter.

4. Experimental results

4.1. FMR spectra

The FMR spectra of a virgin sample and of samples annealed for various times at 375° C are shown in Fig. 1. The resonance curve of the amorphous phase AB in Figs. 1a to d is the only one that can be seen for short ageing times. For ageing times longer than 50 min at 375° C, a second curve appears, whose positive peak is indicated by C in Figs. 1c and d. The negative peak cannot be observed because it is masked by peak B of the amorphous phase. The amplitude and linewidth of this second curve increase with ageing time: for long ageing times, it dominates the spectrum. At the same time, the second curve becomes so broad that the positive peak disappears. The negative peak, however, becomes visible. This peak is indicated by D in Fig. 1e.

4.2. Linewidth measurements

The peak to peak linewidth, ΔH_{pp}, of curve AB is shown in Figs. 2 and 3 as a function of annealing time, for four ageing temperatures between 350 and 375° C. For short annealing times (Fig. 2), the linewidth first decreases, goes through a minimum of about 11.5 mT and then starts to increase. For medium ageing times (Fig. 3) ΔH_{pp} increases very quickly with ageing time. For long ageing times (Fig. 3), the linewidth increases more slowly and tends to a constant value of about 70 mT.

5. Analysis

5.1. Short ageing times

For short ageing times, the linewidth of curve AB decreases with ageing time (Fig. 2). This is attributed to the reorientation of magnetic dipoles in the amorphous material (see Section 2). In other metallic glasses, such as Metglas 2826, with composition $Fe_{40}Ni_{40}P_{14}B_6$ [7], and the amorphous alloy $Fe_{40}Ni_{40}B_{20}$ [8], this relaxation process occurs in two stages, with different time constants. For the annealing temperatures used in this work (350 to 375° C), the first stage of relaxation probably occurs too fast to be measured. The second stage of relaxation was analysed assuming that the process can be described by a first-order kinetic equation, as in other metallic glasses [7–9]. In that case, in terms of the linewidth ΔH_{pp}, the kinetic equation can be written in the form

$$\ln (\Delta H_{pp} - \Delta H_{LL}) = c - kt, \quad (4)$$

where c is a constant and ΔH_{LL} is the Landau–Lifshitz linewidth, given by Equation 2.

The value of ΔH_{LL} was determined by fitting Equation 4 to the experimental data for three ageing temperatures: 350, 359 and 367° C, (for 375° C, the relaxation process is too fast to be measured with any accuracy). Fig. 4 shows, as an example, the fitting for samples annealed at 359° C. The experimental values of c and k in Equation 4 are shown in Table I for the three temperatures investigated. The average value of the Landau–Lifshitz linewidth was $\Delta H_{LL} = 11.3$ mT.

TABLE I Experimental values of the coefficients c and k in Equation 4

T(° C)	c	k(min^{-1})
350	1.474	0.033 66
359	1.582	0.037 66
367	1.563	0.056 76

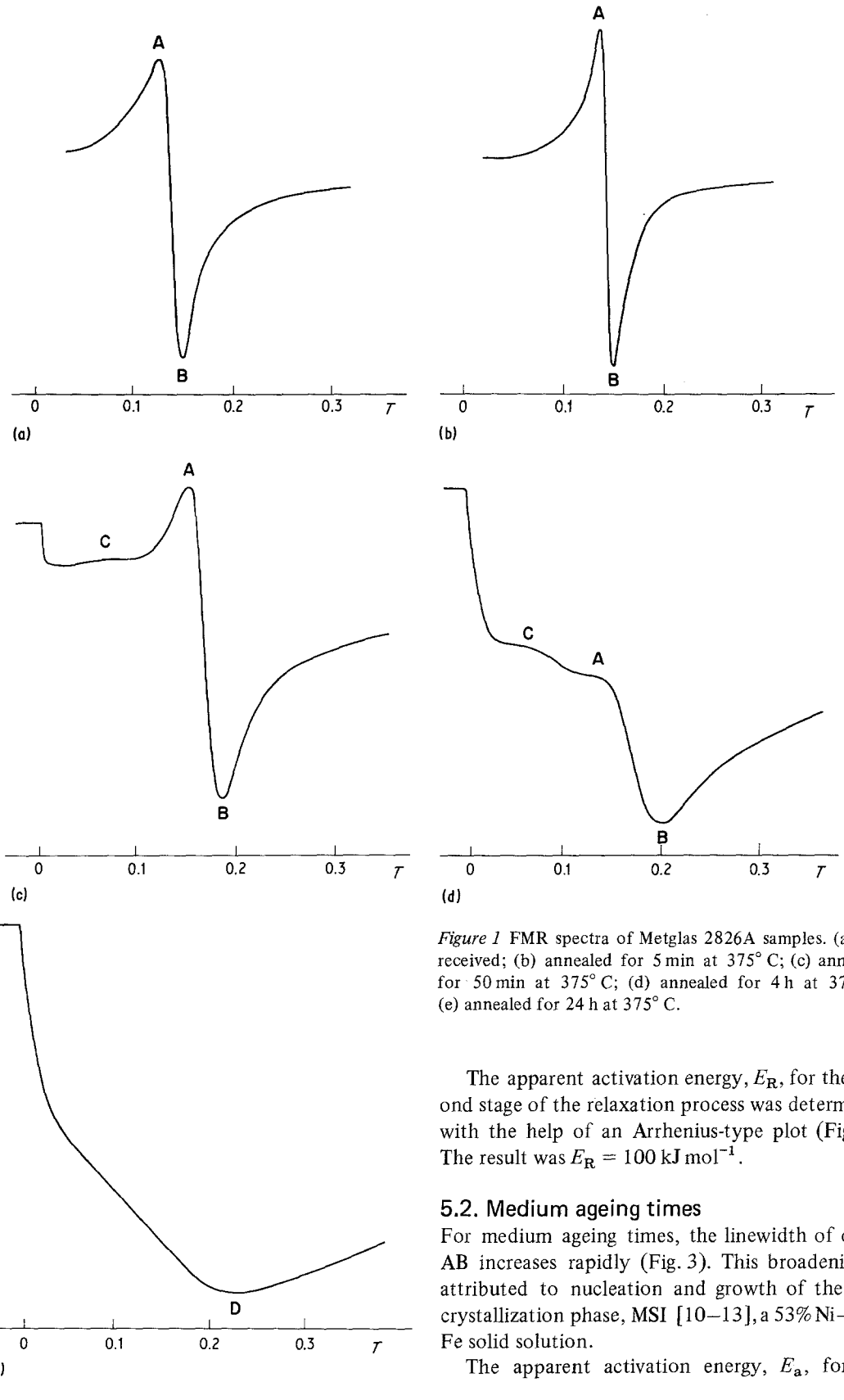

Figure 1 FMR spectra of Metglas 2826A samples. (a) As-received; (b) annealed for 5 min at 375° C; (c) annealed for 50 min at 375° C; (d) annealed for 4 h at 375° C; (e) annealed for 24 h at 375° C.

The apparent activation energy, E_R, for the second stage of the relaxation process was determined with the help of an Arrhenius-type plot (Fig. 5). The result was $E_R = 100\,\text{kJ mol}^{-1}$.

5.2. Medium ageing times

For medium ageing times, the linewidth of curve AB increases rapidly (Fig. 3). This broadening is attributed to nucleation and growth of the first crystallization phase, MSI [10–13], a 53% Ni–47% Fe solid solution.

The apparent activation energy, E_a, for the

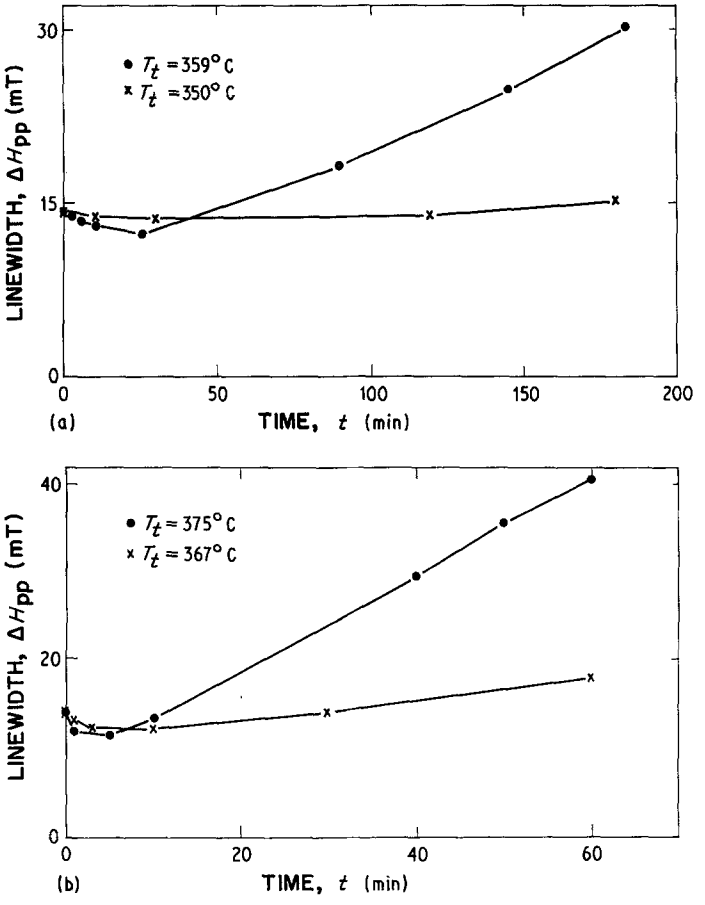

Figure 2 Linewidth of line AB as a function of annealing time, for short annealing times. Samples annealed at (a) 350 and 359° C and (b) 367 and 375° C.

crystallization of phase MSI cannot be determined from a first-order kinetic equation, because the reaction is non-homogeneous [13]. The activation energy was calculated from the temperature dependence of the time to a certain value of the linewidth, $t_{\Delta H}$, according to the equation

$$t_{\Delta H} = A \exp(-E_a/kT), \quad (5)$$

where A is a constant and E_a is the activation energy.

Plots of $\ln t_{\Delta H}$ as a function of $1/T$ are shown in Fig. 6 for several linewidths. The corresponding values of E_a, as obtained from the slopes of straight-line fits to the experimental points, are shown in Table II. The measured activation energy is reasonably constant for linewidths up to 30 mT, with an average value $E_a \simeq 306\,\text{kJ mol}^{-1}$. The reason for the increase in the apparent activation energy for larger linewidths will be discussed in the following section.

5.3. Long ageing times

For long ageing times, the linewidth of Curve AB increases more slowly (Fig. 3); at the same time, a new line, CD, appears in the spectrum (Figs. 1c to e). This is attributed to a second crystallization phase, MSII [10, 11], with composition $(Ni,Fe,Cr)_3(P,B)$. The activation energy of this second phase cannot be determined from linewidth measurements because the corresponding resonance line is so broad that its positive peak is not observed (Fig. 1e) except for a narrow range of ageing times (between 1 and 4 h at 375° C; see Figs. 1c and d).

TABLE II Experimental values of the apparent activation energy of phase MSI, E_a, for several values of the linewidth, ΔH_{pp}

ΔH_{pp}(mT)	E_a(kJ mol^{-1})
15	309
20	303
25	305
30	306
40	334
50	397
60	433

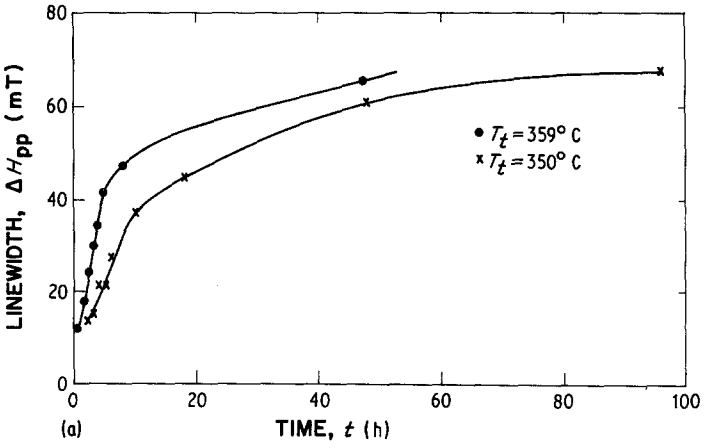

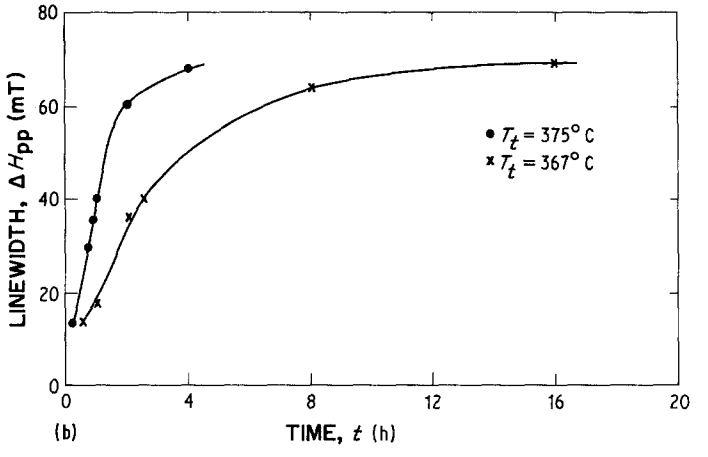

Figure 3 Linewidth of line AB as a function of annealing time, for long annealing times. Samples annealed at (a) 350 and 359° C and (b) 376 and 375° C.

6. Discussion

6.1. Structural relaxation

The process of structural relaxation in metallic glasses has been studied by several researchers [4, 5, 7–9, 14] using different techniques. A comparison between the activation energy, E_R, measured in the present work and the activation energy for the second stage of relaxation in other metallic glasses is shown in Table III. The activation energy for Metglas 2826A is of the same order as that of the alloy $Fe_{40}Ni_{40}B_{20}$ and about twice as large as that of $Fe_{40}Ni_{40}P_{14}B_6$ (Metglas 2826). This suggests that chromium and phosphorus additions have opposite effects on the process of structural relaxation.

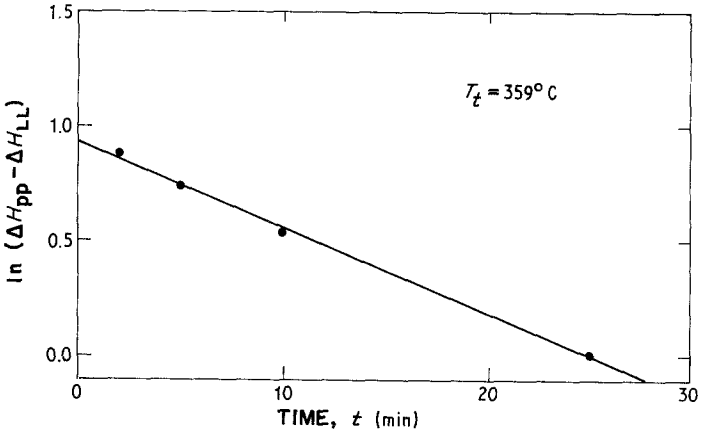

Figure 4 Plot of ln $(\Delta H_{pp} - \Delta H_{LL})$ as a function of annealing time. The straight line is a least-squares fit to the experimental points.

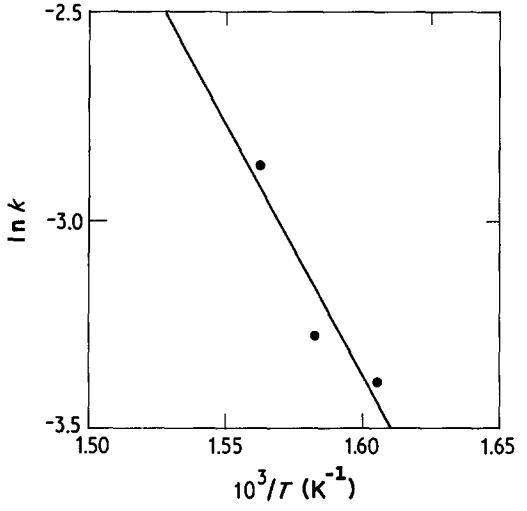

Figure 5 Arrhenius plot for the second stage of the relaxation process.

6.2. MSI phase

As was seen in the preceding section, the broadening of curve AB for medium ageing times is attributed to nucleation and growth of the crystalline phase, MSI. The measured activation energy is compared with the results obtained by other researchers in Table IV. The agreement is fair.

The fact that the activation energy as measured by FMR is in reasonable agreement with data obtained using different methods is an indication that there is indeed a well-defined relation between the linewidth of curve AB and the transformed fraction of phase MSI. In order to determine the form of the relationship, the linewidth for several ageing times and temperatures was plotted against the transformed fraction of phase MSI, as measured by Heimendahl and Maussner using TEM [10]. The result is shown in Fig. 7. The relationship is approximately linear and is the same for all temperatures investigated. A straight-line fit to the data points, assuming that $\Delta H_{pp} = \Delta H_{LL} = 11.3$ mT for $f = 0$ (see Section 5.1) yields the equation

TABLE III Experimental values of the apparent activation energy of the second stage of structural relaxation, E_R, for three metallic glasses

Composition	E_R(kJ mol^{-1})	Reference
$Fe_{32}Ni_{36}Cr_{14}P_{12}B_6$ (Metglas 2826A)	100	Present Work
$Fe_{40}Ni_{40}P_{14}B_6$ (Metglas 2826)	46	[7]
$Fe_{40}Ni_{40}B_{20}$	96	[8]

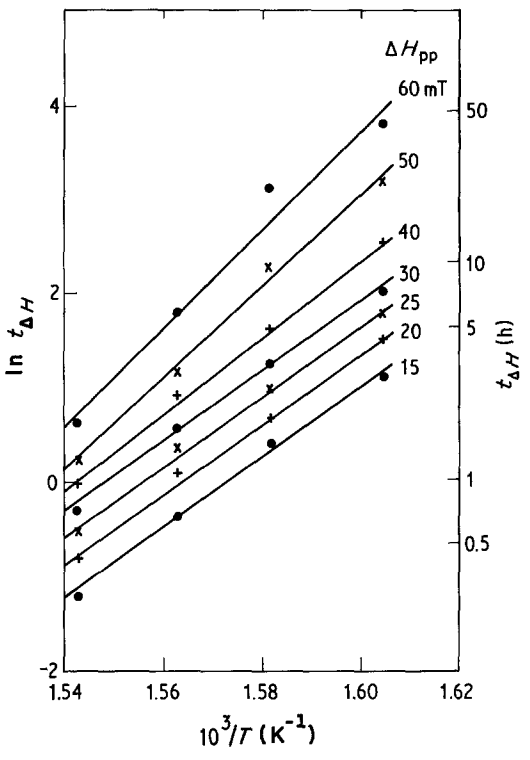

Figure 6 Plot of ln $t_{\Delta H}$ as a function of inverse annealing temperature. The straight lines are least-squares fits to the experimental points.

$$\Delta H_{pp} = 11.3 + 57.0f, \qquad (6)$$

where f is the transformed fraction of phase MSI and ΔH_{pp} is the linewidth in mT.

Once the relationship between ΔH_{pp} and f is known, it is possible to determine the Avrami exponent, n, for the transformation. To do that, the parameters n and k in the Avrami equation

$$f = 1 - \exp[-(kt)^n], \qquad (7)$$

were chosen so as to give the best fit to the experimental points, calculated using Equation 6 to determine the transformed fraction from linewidth data. The results are shown in Fig. 8 and Table V. As can be seen in Fig. 8, the transformed fraction satisfies the Avrami equation up to a transformed fraction of about 50%. The

TABLE IV Experimental values of the apparent activation energy of phase MSI, E_a, as measured by different methods

Experimental method	E_a(kJ mol^{-1})	Reference
FMR	306 ± 25	Present Work
TEM	270 ± 22	[10]
DSC	286	[15]

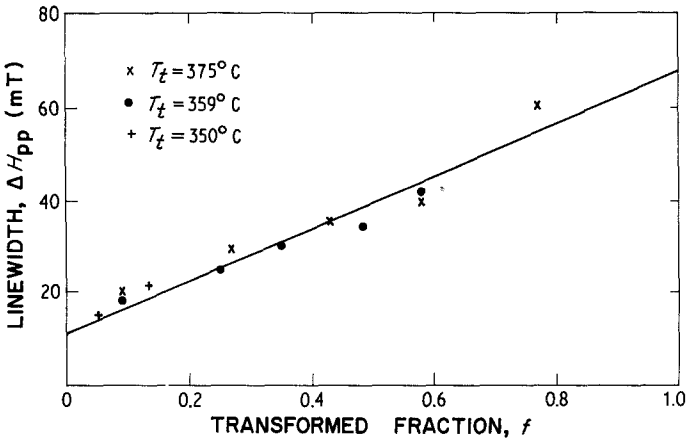

Figure 7 Linewidth of line AB as a function of the transformed fraction of phase MSI, as measured by TEM [10], for three annealing temperatures. The straight line is a least-squares fit to the experimental data, drawn through the point $f = 0$, $\Delta H_{pp} = 11.3$ mT.

experimental results in Table V were obtained by least-squares fitting, using only the experimental points for $f < 0.5$. The average value of n for all annealing temperatures is 1.65, close to the value of 1.7 reported by Heimendahl and Maussner [10] and to the theoretical value of 1.67 proposed by Ilschner [16].

With the help of Equation 7 and using the results in Table V, the transformed fraction as a function of annealing time may be plotted. This is shown in Fig. 9 for three annealing temperatures. The figure also shows the experimental points obtained from linewidth data, using Equation 6, as well as by TEM [10]. For small and medium transformed fractions, the agreement between the theoretical curves and both sets of experimental data is fair; for large transformed fractions, however, the actual transformed fraction is less than its theoretical value. The reason for this discrepancy is discussed below.

6.3. MSII phase

As seen in Section 4, for long annealing times the FMR spectrum shows an absorption line (CD) broader than line AB (see Figs. 1d and e). This line is attributed to a second crystallization phase, MSII. The existence of a second crystalline phase may help to explain two anomalies that were found in the analysis of the data for phase MSI: the increase in the apparent activation energy for $\Delta H_{pp} > 40$ mT (Section 5.2) and the difference between the experimental and theoretical values of the transformed fraction for $f > 0.5$ (Section 6.2). In fact, according to Equation 6, a linewidth $\Delta H_{pp} = 40$ mT corresponds to a transformed fraction of about 0.5, so that both anomalies appear for transformed fractions of phase MSI larger than 50%. It is for transformed fractions of the order of 50% that line CD begins to appear in the FMR spectra. It is thus reasonable to assume that MSII particles start to form when the

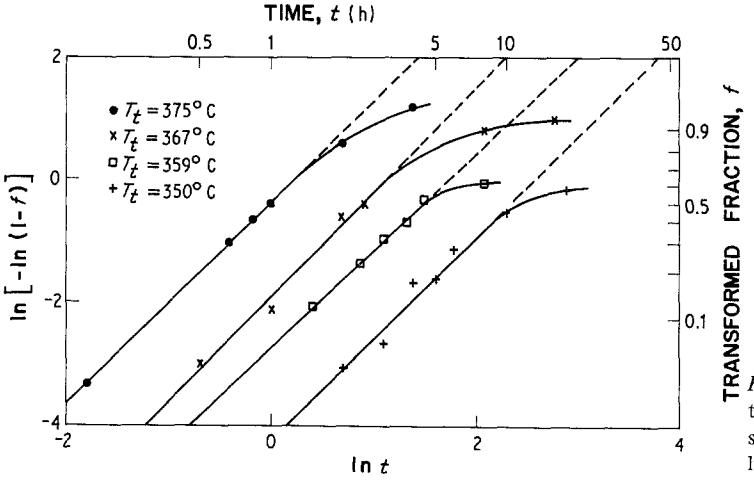

Figure 8 Avrami plots for four annealing temperatures. The straight lines are least-squares fits to experimental points with $\ln[-\ln(1-f)] < 0$.

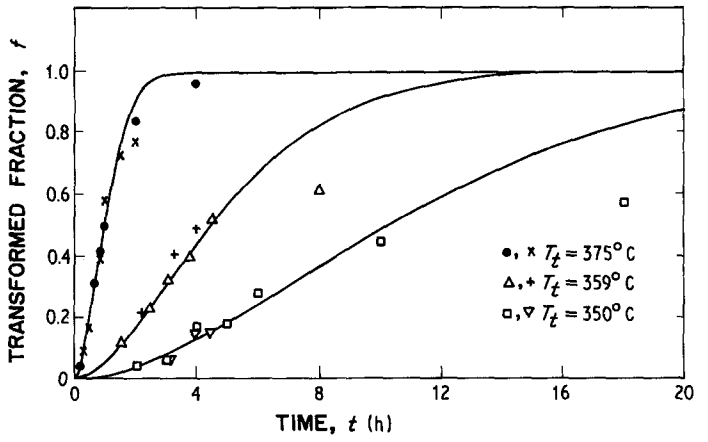

Figure 9 Transformed fraction of phase MSI as a function of annealing time. The curves are theoretical (Equation 7). Experimental points: •, △, □, measured by FMR (present work); x, +, ▽, measured by TEM [10].

transformed fraction of phase MSI is about 50% and that nucleation of phase MSII inhibits the growth of phase MSI particles. This is probably due to the fact that the phases have different compositions [11, 12]. As the particles of phase MSI (which is an Fe–Ni solid solution) nucleate and grow, the amorphous matrix becomes enriched in chromium, phosphorus and boron. Phase MSII presumably starts to form when the concentration of these elements reaches a certain critical value. This is consistent with the fact that when phase MSII starts to form, the crystallites of phase MSI do not dissolve, but are embedded in the crystallites of phase MSII [11].

6.4. The FMR spectrum of phase MSI

A final word should be said about the FMR spectra shown in this work. The spectrum observed in virgin samples (line AB in Fig. 1a) is certainly due to the amorphous phase. According to the interpretation proposed here, line AB becomes narrower (Fig. 1b) for short annealing times due to structural relaxation; for longer ageing times, the line broadens due to the influence of phase MSI crystallites. The broader line (CD) which appears for transformed fractions of phase MSI larger than 50% (Figs. 1c to e) is attributed to phase MSII. Where, then, is the spectrum due to phase MSI crystallites? There are two possible explanations: either phase MSI particles are antiferromagnetic, weakly ferromagnetic or paramagnetic (in that case, the spectrum would be too weak to be seen) or line AB in annealed samples is a superposition of the spectra of the amorphous phase and of MSI particles. The fact that the intensity of line AB increases with annealing time up to large transformed fractions of phase MSI seems to rule out the first hypothesis. On the other hand, the resonance fields of the amorphous phase and of phase MSI are expected to be almost equal, since both phases have the same short-range order, as shown by TEM diffraction patterns of virgin and annealed samples [17]. In addition, the inhomogeneity of the internal magnetic field caused by nucleation and growth of the crystallites, should affect both lines in the same way. We are thus led to the conclusion that line AB is probably the sum of two lines, one due to the amorphous phase and the other due to MSI crystallites.

TABLE V Experimental values of the Avrami exponent, n, and the reaction rate, k, for the crystallization of phase MSI

T(° C)	n	k(h^{-1})
350	1.66	0.08
359	1.58	0.18
367	1.71	0.34
375	1.66	0.82

Acknowledgements

The authors thank Dr M. von Heimendahl, who provided the virgin samples used in this work, Dr P. D. Portella, who performed part of the heat treatments, Dr R. Pascual and Dr T. C. Devezas, for many helpful discussions. This work was carried out with financial support from FINEP, CNPq (Pronuclear) and Ministério do Exército.

References

1. G. V. SKROTSKII and K. V. KURBATOV, in "Ferromagnetic Resonance", edited by S. V. Vonsovskii (Pergamon Press, Oxford, 1966).
2. S. CHIKAZUMI, "Physics of Magnetism" (John Wiley, New York, 1964) Ch. 16.

3. C. VITTORIA, P. LUBITZ and V. RITZ, *J. Appl. Phys.* **49** (1978) 4908.
4. I. C. BAIANU, K. A. RUBINSON and J. PATTERSON, *J. Phys. Chem. Solids* **40** (1979) 941.
5. I. C. BAIANU, J. PATTERSON and K. A. RUBINSON, *Mater. Sci. Eng.* **40** (1979) 273.
6. E. FIGUEROA, L. LUNDGREN, O. BECKMAN and S. M. BHAGAT, *Solid State Commun.* **20** (1976) 961.
7. F. E. LUBORSKY and J. L. WALTER, *Mater. Sci. Eng.* **35** (1978) 255.
8. G. C. CHI, H. S. CHEN and C. E. MILLER, *J. Appl. Phys.* **49** (1978) 1715.
9. H. S. CHEN, *Rep. Prog. Phys.* **43** (1980) 353.
10. M. VON HEIMENDAHL and G. MAUSSNER, Proceedings of the Third International Conference on Rapidly Quenched Metals, Vol. I, Brighton, London, 1978 (The Metals Society, London, 1978) p. 424.
11. *Idem, J. Mater. Sci.* **14** (1979) 1238.
12. M. VON HEIMENDAHL and H. OPPOLZER, *Scripta Metall.* **12** (1978) 1027.
13. M. VON HEIMENDAHL and G. KUGLSTATTER, *J. Mater. Sci.* **16** (1981) 2405.
14. C. D. GRAHAM Jr, T. EGAMI, R. S. WILLIAMS and Y. TAKEI, *AIP Conf. Proc.* **29** (1976) 218.
15. C. ANTONIONE, L. BATTEZZATI, A. LUCCI, G. RIONTINO and G. VENTURELLO, *Scripta Metall.* **12** (1978) 1011.
16. B. ILSCHNER, *Arch. Eisenhuttenw.* **26** (1955) 59.
17. R. PASCUAL, private communication (1983).

Received 14 February
and accepted 6 April 1984